Induction of Core Circadian Clock Transcription Factor Bmal1 Enhances β-Cell Function and Protects Against Obesity-Induced Glucose Intolerance

Kuntol Rakshit[1] and Aleksey V. Matveyenko[1,2]

Diabetes 2021;70:143–154 | https://doi.org/10.2337/db20-0192

Type 2 diabetes mellitus (T2DM) is characterized by β-cell dysfunction as a result of impaired glucose-stimulated insulin secretion (GSIS). Studies show that β-cell circadian clocks are important regulators of GSIS and glucose homeostasis. These observations raise the question about whether enhancement of the circadian clock in β-cells will confer protection against β-cell dysfunction under diabetogenic conditions. To test this, we used an approach by first generating mice with β-cell–specific inducible overexpression of *Bmal1* (core circadian transcription factor; *β-Bmal1*^{OV}). We subsequently examined the effects of *β-Bmal1*^{OV} on the circadian clock, GSIS, islet transcriptome, and glucose metabolism in the context of diet-induced obesity. We also tested the effects of circadian clock–enhancing small-molecule nobiletin on GSIS in mouse and human control and T2DM islets. We report that *β-Bmal1*^{OV} mice display enhanced islet circadian clock amplitude and augmented in vivo and in vitro GSIS and are protected against obesity-induced glucose intolerance. These effects were associated with increased expression of purported BMAL1-target genes mediating insulin secretion, processing, and lipid metabolism. Furthermore, exposure of isolated islets to nobiletin enhanced β-cell secretory function in a *Bmal1*-dependent manner. This work suggests therapeutic targeting of the circadian system as a potential strategy to counteract β-cell failure under diabetogenic conditions.

The circadian system is a critical component of mammalian homeostasis, permitting organismal fitness in response to 24-h environmental cycles (1). A key aspect of circadian physiology is its intrinsic nature, that is, the presence of internal circadian oscillators (or clocks) that exert control over diverse physiological, genetic, and metabolic cellular functions (2). Intrinsic β-cell circadian clocks are important regulators of glucose-stimulated insulin secretion (GSIS), β-cell maturation, turnover, and response to diabetogenic stressors (3–8). Therefore, evidence links circadian disruption with development of type 2 diabetes mellitus (T2DM) (9–11), and recent studies show perturbations of intrinsic β-cell clocks in human islets of patients with T2DM (12).

At the molecular level, circadian clocks are governed by a genetic feedback loop comprising transcriptional activators brain and muscle ARNT-like 1 (BMAL1) (*Arntl/Bmal1*) and its heterodimeric partner CLOCK and repressor genes that encode period (PER) and cryptochrome (CRY) proteins (2). BMAL1 is a key circadian transcriptional regulator since it is a nonredundant clock gene indispensable for the generation of circadian rhythms (13). BMAL1 predominantly regulates transcription of genes in a tissue-specific manner; however, transcripts commonly regulated by BMAL1 are enriched for pathways regulating glucose homeostasis (14). In β-cells, purported BMAL1 targets mediate critical aspects of insulin secretion, exocytosis, and metabolism (6). Consistently, β-cell–specific *Bmal1* deletion in mice (or *BMAL1* genetic variance in humans) is associated with β-cell failure, glucose intolerance, and T2DM (3,15–17).

These observations raise the question of whether enhancement of the circadian clock (and specifically BMAL1 expression) selectively in β-cells will confer protection against β-cell dysfunction in response to diabetogenic stressors common to T2DM. In support of this premise,

[1]Department of Physiology and Biomedical Engineering, Mayo Clinic School of Medicine, Rochester, MN
[2]Division of Endocrinology, Metabolism, Diabetes, and Nutrition, Department of Medicine, Mayo Clinic School of Medicine, Rochester, MN
Corresponding author: Aleksey V. Matveyenko, matveyenko.aleksey@mayo.edu

Received 25 February 2020 and accepted 15 October 2020

This article contains supplementary material online at https://doi.org/10.2337/figshare.13103045.

recent studies have shown that treatment of rodents with pharmacological enhancers of circadian rhythms improves glucose homeostasis in the context of obesity, diabetes, and circadian disruption (18,19). Although these studies support the premise that enhancement of the circadian clock may be effective in the treatment of T2DM, whether clock-enhancing strategies can be effective in counteracting β-cell failure in vivo requires further investigation.

In this study, we provide evidence that enhancement of β-cell circadian clock in vivo (through conditional β-cell–specific overexpression of *Bmal1*) augments GSIS and glucose tolerance in context of diet-induced obesity and insulin resistance. Importantly, beneficial effects of β-cell *Bmal1* induction were associated with increased expression of genes mediating insulin secretion, lipid metabolism, and endoplasmic reticulum (ER) function. Moreover, pharmacological enhancement of circadian clocks (with small-molecule nobiletin) was shown to improve GSIS in isolated mouse and human islets, implicating therapeutic targeting of circadian clocks for treatment of diabetes.

RESEARCH DESIGN AND METHODS

Animals

All animal procedures were approved by the Mayo Clinic institutional animal care and use committee. In total, 120 male mice were used for all studies. Mice expressing a hemagglutinin-tagged (HA) copy of *Bmal1* under the control of tetracycline-responsive (tetO) promoter (B6.Cg-Tg[tetO-Arntl]1Jt/J, #007618; The Jackson Laboratory) (20), were crossed to mice that express the reverse tetracycline-controlled transactivator protein (rtTA) under the control of rat insulin 2 promoter (Tg[Ins2-rtTA]2Efr/J, #008250; The Jackson Laboratory) (21). Resulting offspring were genotyped to identify mice containing both tetO promoter and rtTA transactivator $Bmal1\text{-}HA^{tetO/+}Ins2^{rtTA/+}$ (referred to as $\beta\text{-}Bmal1^{OV}$) or littermate controls containing the rtTA transactivator $^{+/+}Ins2^{rtTA/+}$ (referred to as control) alone. For assessment of circadian clock function in $\beta\text{-}Bmal1^{OV}$ mice, additional mice were generated by crossing $Bmal1^{tetO/+}Ins2^{rtTA/+}$ mice to homozygous $mPer2^{luc}$ knockin mice, which express mouse *Per2*:luciferase (*Per2*:LUC) reporter (B6.129S6-$Per2^{tm1Jt}$/J, #006852; The Jackson Laboratory). Offspring were genotyped to identify $^{+/+}Ins2^{rtTA/+}Per2^{luc/+}$ and $Bmal1^{tetO/+}Ins2^{rtTA/+}Per2^{luc/+}$ mice (referred to as control-LUC and $\beta\text{-}Bmal1^{OV}$-LUC, respectively). To assess the effect of nobiletin on β-cell circadian clock, *Per2*:LUC reporter mice were bred with mice expressing green fluorescent protein (GFP) under the control of the insulin 1 promoter (B6.Cg-Tg[Ins1-EGFP], #006864; The Jackson Laboratory) (22). Resulting offspring were subsequently referred to as $Per2^{luc/+}Ins1^{GFP/+}$. Mice with β-cell–specific deletion of *Bmal1* (referred to as $\beta\text{-}Bmal1^{-/-}$) were generated by breeding mice homozygous for the floxed Bmal1 gene (B6.129S4 [Cg]-$Arntl^{tm1Weit}$/J; The Jackson Laboratory) (23) with mice transgenic for tamoxifen-inducible Cre driven by the rat Insulin2 promoter (Tg [*Ins2*-cre/ERT]; The Jackson Laboratory) (24). To activate deletion of *Bmal1*, $\beta\text{-}Bmal1^{-/-}$ mice received three i.p. injections of 4 mg tamoxifen (Sigma-Aldrich) as previously described (16).

Experimental Design for In Vivo Studies

All mice were housed under a standard 12-h light, 12-h dark (LD) cycle. By convention, the time of lights on (0600 h) is denoted as Zeitgeber time (ZT) 0 and time of lights off (1800 h) as ZT 12. Mice were fed chow (Harlan Laboratories, Indianapolis, IN) until the age of 2 months, following which time they were switched to doxycycline (DOX) diets to achieve *Bmal1* overexpression in β-cells. On the basis of the experimental design, mice were fed either chow (9% fat, 20% protein, 54% carbohydrates, 200 mg · kg^{-1} DOX, S3888; Bio-Serv, Flemington, NJ) or 60% high-fat diet (HFD) (60% fat, 20% protein, 20% carbohydrates, 280 mg · kg^{-1} DOX, F7160; Bio-Serv).

Monitoring of Circadian Activity and Metabolic Rate

Mice were housed in cages fitted with an optical beam sensor system (Respironics, Murrysville, PA) and monitored for 24 days in LD followed by 48 days in constant darkness (DD). Food consumption and metabolic rate were monitored using a comprehensive laboratory animal monitoring system equipped with an Oxymax open circuit indirect calorimeter system (Columbus Instruments, Columbus, OH).

Assessment of Diurnal Glucose and Insulin Tolerance

To assess glucose tolerance, mice received 1 g · kg^{-1} body weight of 50% dextrose solution through i.p. injection performed at 1000 h (ZT 4, day) and 2200 h (ZT 16, night). Blood glucose was measured at 0, 15, 30, 60, and 90 min post-dextrose injection. At 15 min, blood was sampled through saphenous venipuncture into microcentrifuge tubes for collection of plasma. To assess insulin tolerance, mice received 0.75 mU · g^{-1} body weight of insulin solution through i.p. injection performed at ZT 4, and blood glucose was serially measured at 0, 10, 20, 30, 40, 50, and 60 min post-insulin bolus.

Measurement of β-Cell Function In Vitro by Islet Perifusion

Mouse islets were isolated (always at the ZT 4 time point/1000 h central standard time [CST]) using standard collagenase method and recovered overnight in RPMI medium as previously described (16). Human islets were obtained from Prodo Laboratories (Irvine, CA) and cultured in RPMI medium as previously detailed (25). In total, two independent shipments of nondiabetic (HP-20030 and HP-20164) and one shipment of T2DM (HP-20019) human islets were used and four to six independent perifusion experiments ("runs") were conducted for each shipment. All perifusion experiments (performed always at the ZT 4 time point/1000 h CST) were conducted using a Biorep perifusion system (Biorep Technologies, Miami, FL) as previously described (16). When appropriate, nobiletin (10 μmol · L^{-1}; Toronto Research Chemicals) was diluted in 4 mmol · L^{-1} and 16 mmol · L^{-1} glucose

perifusion buffers and was continuously administered throughout the basal wash (−48 to 0 min) and sample collection period (0–96 min) of islet perifusion.

Assessment of Islet Circadian Clock Ex Vivo Using *Per2* Bioluminescence Reporter

Islets were isolated from either control-LUC ($^{+/+}$*Ins2*$^{rtTA/+}$ *Per2*$^{luc/+}$), *β-Bmal1*^{OV}-LUC (*Bmal1*$^{tetO/+}$*Ins2*$^{rtTA/+}$*Per2*$^{luc/+}$) or *Per2*$^{luc/+}$*Ins1*$^{GFP/+}$ mice at the ZT 4 time point/1000 h CST. Batches of 25 islets were placed in individual wells of Nunc Lab-Tek Chambered Coverglass (Thermo Fisher Scientific, Waltham, MA), each containing RPMI medium with 10% FBS, 0.1 mmol · L^{-1} D-LUCIFERIN (L-8220; Biosynth, Itaska, IL), and nobiletin (10 μmol/L · L^{-1}) (when appropriate). The coverglass-containing islets were placed in the Luminoview LV200 Bioluminescence Imaging System (Olympus, Center Valley, PA) and imaged for 5 days at hourly intervals. Bioluminescence signal was quantified using cellSens software (Olympus). Data were normalized by subtraction of the 24-h running average from raw data and then smoothed with a 2-h running average as previously described (26,27).

Islet RNA Extraction, Quantitative Real-time PCR, and Affymetrix GeneChip

For Affymetrix GeneChip, mouse islets were isolated from seven control-HFD ($n = 3$ at ZT 4 and $n = 4$ at ZT 16) and eight *β-Bmal1*^{OV}-HFD ($n = 5$ at ZT 4 and $n = 3$ at ZT 16) mice. To maximize the amount and quality of RNA, islet samples were pooled to create a sample for each genotype/ZT, and total RNA was extracted using an RNeasy Mini Kit (QIAGEN). RNA was quantified by NanoDrop One^{C} (Thermo Fisher Scientific), and microarray analysis was conducted according to the manufacturer's instructions for the GeneChip WT Pico Reagent Kit (Affymetrix, Santa Clara, CA) as previously described (8). A differentially expressed gene list was subjected to Gene Ontology (GO) enrichment analysis using DAVID (28) and subjected to gene set enrichment analysis (GSEA) using defined BMAL1 chromatin immunoprecipitation sequencing targets (6). For quantitative real-time PCR (qRT-PCR), mRNA was converted into cDNA using an iScript cDNA Synthesis Kit (Bio-Rad, Hercules, CA), and qRT-PCR was performed on the StepOnePlus machine (Applied Biosystems, Carlsbad, CA) under default thermal cycling conditions. Data were analyzed using the $2^{-\Delta\Delta CT}$ method, with mRNA levels normalized to *Actin* and *Gapdh* for every sample.

Immunofluorescence and Endocrine Pancreas Morphology

Paraffin-embedded pancreatic sections were stained for insulin (ab7842; Abcam), glucagon (G2654; Sigma-Aldrich), BMAL1 (ab3350; Abcam), HA (H3663; Sigma-Aldrich), replication marker Ki67 (550609; BD Pharmingen), and apoptosis marker TUNEL (Roche). Slides were viewed using a Zeiss microscope (Carl Zeiss Microscopy) and images acquired using ZEN pro software (Carl Zeiss Microscopy).

Analytical Methods

Blood glucose was measured with a FreeStyle Lite blood glucose measuring system (Abbott Laboratories, Abbott Park, IL). Insulin was measured using Insulin ELISA (ALPCO, Salem, NH).

Statistical Analysis and Calculations

Per2-driven luciferase rhythms were assessed using JTK_CYCLE software version 3 (Hughes Laboratory, Washington University, St. Louis, MO) (29). Activity recordings were analyzed using ClockLab software (Actimetrics, Wilmette, IL). Statistical analysis was performed using ANOVA with post hoc tests wherever appropriate (GraphPad Prism 8.2; GraphPad Software, San Diego, CA). Data in graphs are presented as mean ± SEM and assumed statistically significant at $P < 0.05$.

Data and Resource Availability

The experimental data sets generated and/or analyzed during the current study are available from the corresponding author upon reasonable request. No applicable resources were generated during the current study.

RESULTS

Validation of β-Cell BMAL1 Overexpression in Male Mice

We generated double-transgenic mice with conditional β-cell–specific overexpression of *Bmal1* (*β-Bmal1*^{OV}; *Bmal1-HA*$^{tetO/+}$*Ins2*$^{rtTA/+}$) and corresponding littermate controls (control; $^{+/+}$*Ins2*$^{rtTA/+}$), which were subsequently exposed to either chow or 60% HFD, while *Bmal1* overexpression was driven by provision of DOX in food (Fig. 1*A* and *B*). *Bmal1* in islets demonstrated an expected diurnal expression pattern in control and *β-Bmal1*^{OV} under both chow and HFD, with increased mRNA at ZT 16 (active/dark cycle) (Fig. 1*C*). Interestingly, in control mice, exposure to HFD led to a significant decrease in *Bmal1* mRNA at ZT 4 but augmented *Bmal1* expression at the ZT 16 time point ($P < 0.05$ for chow vs. HFD). HFD did not alter *Bmal1* expression in *β-Bmal1*^{OV} islets, which was robustly increased (~20–40-fold, $P < 0.05$) at both ZT 4 and ZT 16 compared with respective controls (Fig. 1*C*). Immunostaining for insulin, BMAL1, and HA in pancreatic sections confirmed robust induction of BMAL1 protein in insulin-positive cells of *β-Bmal1*^{OV} mice (Fig. 1*D*).

BMAL1 Overexpression in β-Cells Does Not Alter Global Circadian Rhythms in Activity, Feeding, or Metabolism

To confirm the specificity of *Bmal1* overexpression to β-cells, we performed assessment of in vivo circadian rhythms in locomotor activity, feeding, and energy expenditure (Fig. 2). Chow- or HFD-fed control and *β-Bmal1*^{OV} genotypes displayed comparable circadian activity under the standard LD cycle as well as during the free-run DD cycle, exhibiting an ~24-h dominant activity period ($P > 0.05$ between the genotypes) (Fig. 2*A*). In addition, whole-body calorimetry analysis confirmed an expected decrease

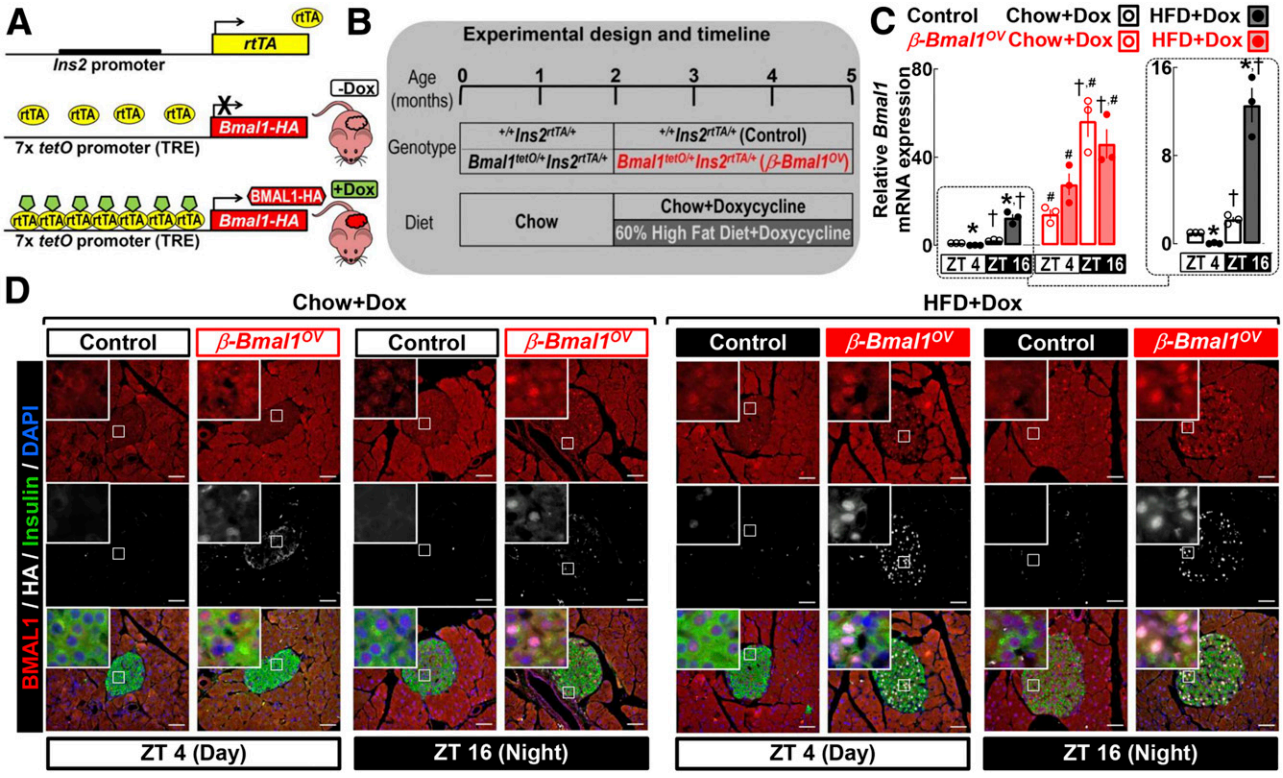

Figure 1—Generation and validation of β-cell *Bmal1* overexpression in male mice. *A* and *B*: We generated mice with conditional β-cell–specific expression of *Bmal1* by crossing mice expressing HA copy of *Bmal1* under the control of tetO promoter (tetO-*Bmal1*-HA) with mice expressing the rtTA under the control of rat insulin promoter (*Ins2*-rtTA). Resultant offspring and corresponding controls were exposed to either chow or 60% HFD, while *Bmal1* expression was driven by provision of DOX in food. *C*: Normalized *Bmal1* mRNA from islet lysates of chow- and HFD-fed control ($^{+/+}Ins2^{rtTA/+}$) and *β-Bmal1*^{OV} ($Bmal1\text{-}HA^{tetO/+}Ins2^{rtTA/+}$) male mice collected at the ZT 4 and ZT 16 time points. Data are mean ± SEM (at least $n = 3$ mice per genotype/diet) fold change, with chow-fed control at ZT 4 set as 1. Statistical significance was determined by three-way ANOVA for effects of genotype, diet, and ZT with post hoc multiple comparison analysis. *$P < 0.05$ for chow vs. HFD; #$P < 0.05$ for control vs. *β-Bmal1*^{OV}; †$P < 0.05$ for ZT 4 vs. ZT 16. *D*: Representative pancreatic sections stained by immunofluorescence for BMAL1, insulin, and HA and counterstained with nuclear marker DAPI imaged at 20× (scale bars = 50 μm) and magnification ×63 (insets) in chow- and HFD-fed control and *β-Bmal1*^{OV} mice at the ZT 4 and ZT 16 time points. In total, representative pancreatic specimens from at least $n = 3$ mice per genotype/diet were examined.

in circadian variation in VO_2, VCO_2, and total metabolic rate in HFD-fed vs. chow-fed animals; however, no differences in any of the metabolic parameters were detected between control and *β-Bmal1*^{OV} mice ($P > 0.05$) (Fig. 2*B*). Control and *β-Bmal1*^{OV} mice also exhibited a comparable increase in body mass and daily food intake in response to HFD (Supplementary Fig. 1). These data confirm that chow- and/or HFD-fed *β-Bmal1*^{OV} mice do not differ from control with respect to the regulation of systemic circadian rhythms, metabolic rate, body weight, or feeding.

BMAL1 Overexpression in β-Cells Enhances Circadian Clock Amplitude in Islets of *Per2*:LUC Reporter Mice

To test the effects of β-cell–specific expression of *Bmal1* on the islet circadian clock, we generated a triple-transgenic mouse by crossing *β-Bmal1*^{OV} mice to homozygous *Per2*:LUC knockin mice (commonly used circadian reporter mouse model [30]). Resulting offspring control-LUC ($^{+/+}Ins2^{rtTA/+}Per2^{luc/+}$) and *β-Bmal1*^{OV}-LUC ($Bmal1^{tetO/+}Ins2^{rtTA/+}Per2^{luc/+}$) were used for bioluminescence recordings of isolated islets (Fig. 3). As expected, islets from chow- and/or HFD-fed control and *β-Bmal1*^{OV} mice displayed sustained circadian rhythms in *Per2* bioluminescence (Fig. 3*A*–*C*). Interestingly, exposure to HFD (independent of the genotype) enhanced the amplitude (~50%, $P < 0.05$ vs. chow) of *Per2*-driven luciferase oscillations, indicative of a potential compensatory increase in the circadian clock amplitude in response to HFD. Importantly, the amplitude of *Per2*-driven luciferase oscillations was further augmented in islets of HFD-fed *β-Bmal1*^{OV} mice compared with control (~50%, $P <$ 0.05 vs. HFD-control) (Fig. 3*C*). Consistently, qRT-PCR performed on islets isolated at multiple time points during the LD cycle (e.g., ZT 4, 8, 16, and 20) confirmed robust upregulation in diurnal *Bmal1* mRNA as well as increased diurnal expression in *Per2* and *Nr1d1* mRNA in HFD-fed *β-Bmal1*^{OV} compared with control mice ($P <$ 0.05) (Fig. 3*D*). Collectively, these data demonstrate that *β-Bmal1*^{OV} mice exhibit enhancement of islet circadian clock amplitude and clock gene expression under HFD conditions.

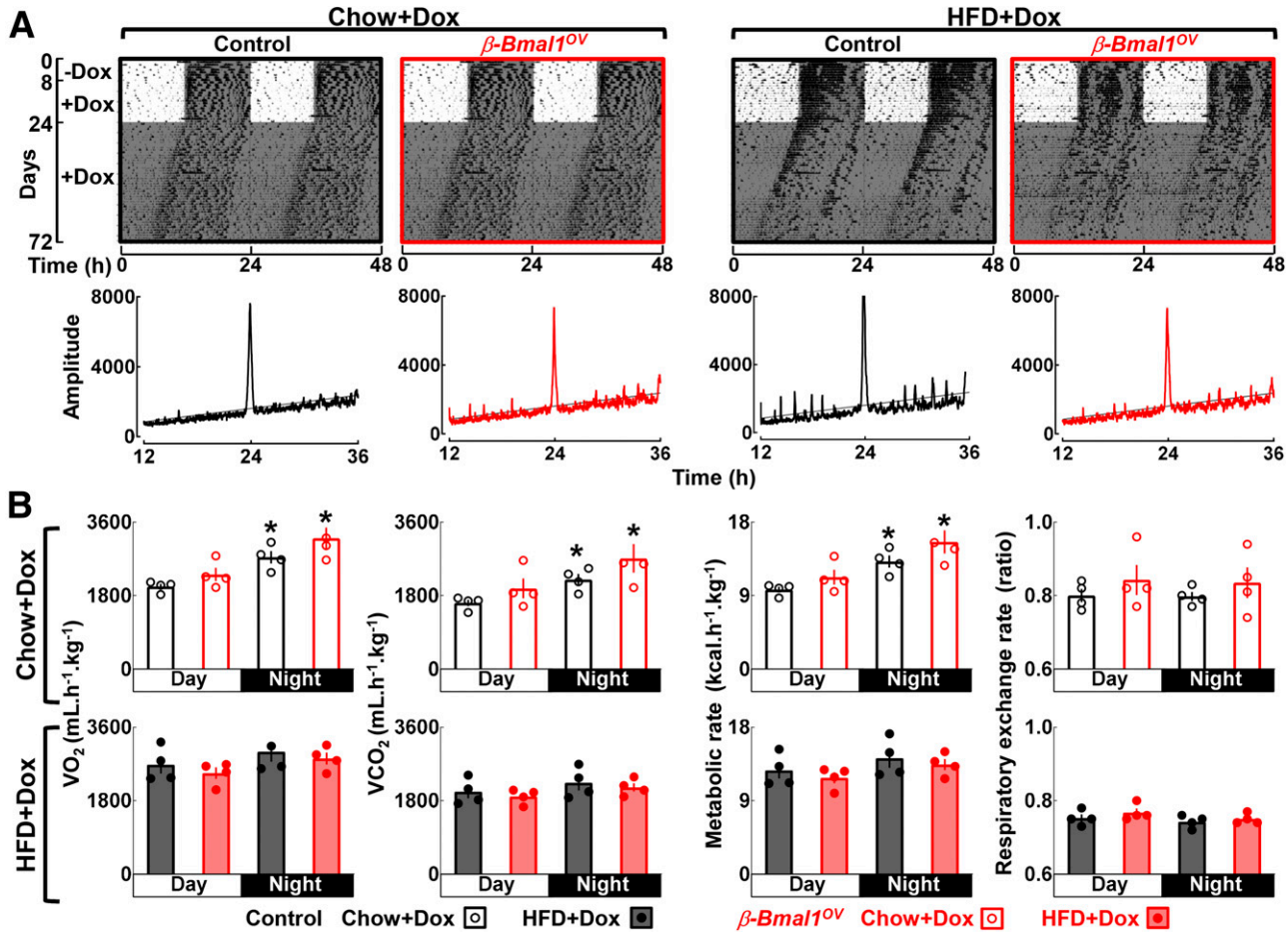

Figure 2—*Bmal1* overexpression in β-cells does not alter global regulation of circadian rhythms in activity and energy expenditure in male mice. *A*: Representative actograms (double plotted) of locomotor activity in chow- and HFD-fed control ($^{+/+}$*Ins2*$^{rtTA/+}$) and *β-Bmal1*^{OV} (*Bmal1-HA*$^{tetO/+}$*Ins2*$^{rtTA/+}$) male mice monitored for 8 days in a standard LD cycle without DOX followed by 16 days in LD and 48 days in DD with DOX administration (200 mg · kg^{-1} in food). Shaded areas represent periods of dark. Corresponding χ^2 periodograms of activity recordings are shown below each actogram. In total, activity patterns were examined in $n = 4$ mice per genotype/diet. *B*: Average measurements of VO_2, VCO_2, metabolic rate, and the respiratory exchange ratio (RER) monitored over a 24-h period in chow-fed and HFD-fed control and *β-Bmal1*^{OV} mice. Calorimetric recordings were made using a comprehensive laboratory animal monitoring system . VO_2 and VCO_2 levels were used to calculate the RER, and VO_2 and RER values were used to determine the metabolic rate (kcal · kg^{-1} · h^{-1}). Data are mean ± SEM ($n = 4$ mice per genotype/diet). *$P < 0.05$ vs. day cycle.

BMAL1 Overexpression in β-Cells Enhances In Vivo Glucose Tolerance in Response to Diet-Induced Obesity

We next performed glucose tolerance tests (GTTs) with concomitant measure of in vivo glucose-stimulated insulin in chow- and HFD-fed control and *β-Bmal1*^{OV} mice at the ZT 4 and ZT 16 time points (Fig. 4). Before the administration of DOX and/or HFD, control and *β-Bmal1*^{OV} mice displayed comparable glucose tolerance (Fig. 4*A–D*, baseline). As expected, HFD-fed controls demonstrated induction of glucose intolerance evident by approximately two- and threefold increases in glucose area under the curve (AUC) during GTT at the ZT 4 and 16 time points ($P < 0.05$ for control HFD vs. chow) (Fig. 4). Strikingly, at ZT 4, HFD-fed *β-Bmal1*^{OV} mice demonstrated the same degree of glucose tolerance as their chow-fed counterparts, indicating protection from HFD-induced glucose intolerance ($P > 0.05$ for *β-Bmal1*^{OV} HFD vs. chow) (Fig. 4). At ZT 16, HFD-fed *β-Bmal1*^{OV} exhibited mild glucose intolerance ($P < 0.05$ for HFD vs. chow); however, the extent of glucose intolerance was significantly attenuated compared with controls ($P < 0.05$ for *β-Bmal1*^{OV} vs. control). Of note, improved glucose tolerance in HFD-fed *β-Bmal1*^{OV} mice was attributed to enhanced insulin levels and response ($P < 0.05$ for *β-Bmal1*^{OV} vs. control at ZT 4) (Fig. 4*D*), with no change in insulin sensitivity (Supplementary Fig. 2).

BMAL1 Overexpression in β-Cells Enhances In Vitro β-Cell Function Without Altering β-Cell Mass and/or Turnover in Response to Diet-Induced Obesity

Consistent with previous observations (31,32), islet perifusion studies (performed at ZT 4) revealed that islets

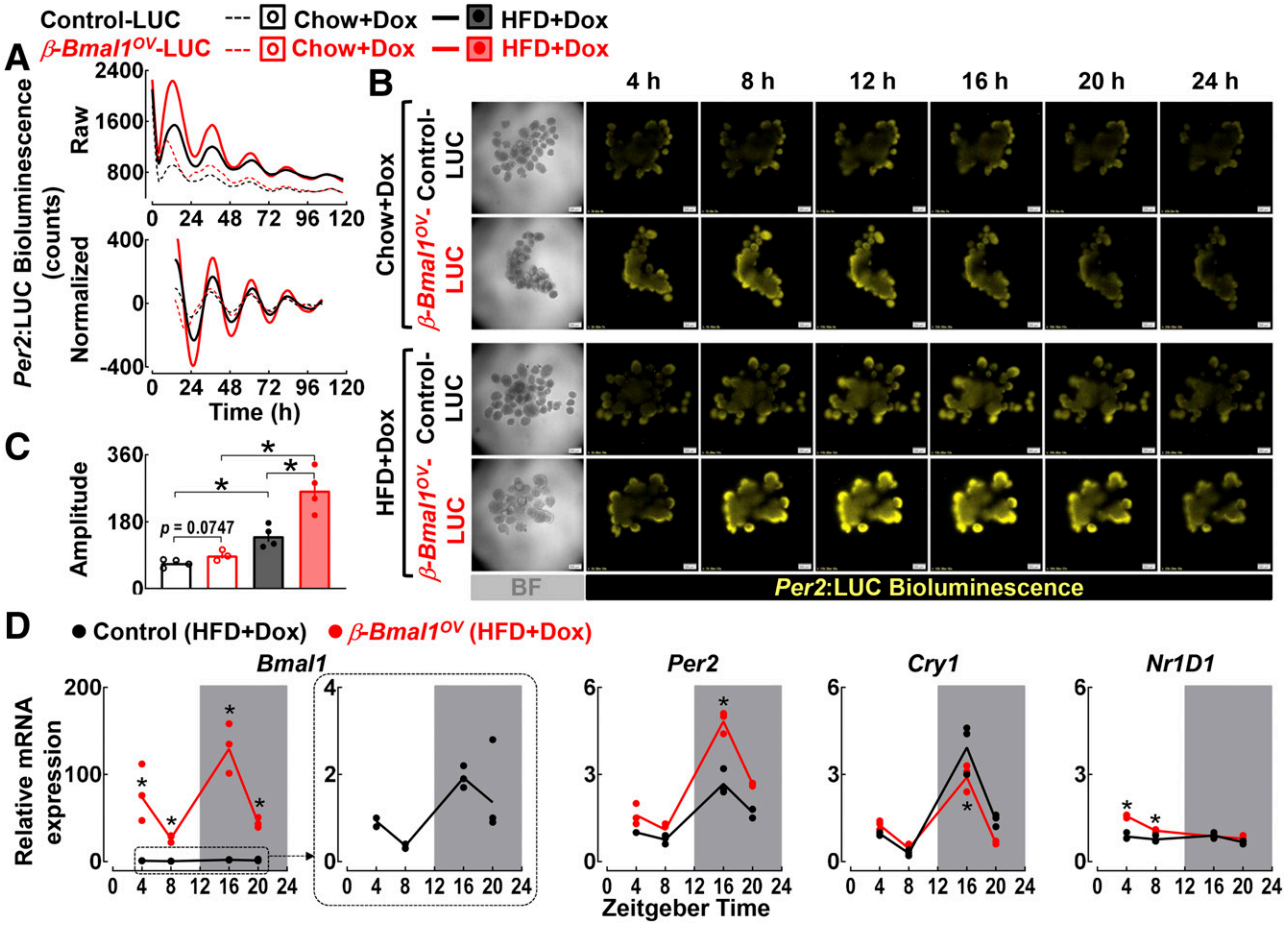

Figure 3—β-Cell *Bmal1* overexpression enhances islet circadian clock amplitude in *Per2*:LUC reporter male mice. *A*: Representative examples of *Per2*-driven bioluminescence rhythms (raw and normalized counts). *B*: Twenty-four hours of time-lapse microscopy recordings in islets isolated from control-LUC ($^{+/+}Ins2^{rTtA/+}Per2^{luc/+}$) and *β-Bmal1*^{OV}-LUC (*Bmal1-HA*$^{tetO/+}$$Ins2^{rTtA/+}Per2^{luc/+}$) mice exposed to either chow or HFD (scale bars = 200 μm). *C*: Mean circadian amplitude of *Per2*-driven bioluminescence rhythms in islets of chow or HFD-fed control ($^{+/+}Ins2^{rTtA/+}Per2^{luc/+}$) and *β-Bmal1*^{OV} (*Bmal1-HA*$^{tetO/+}$$Ins2^{rTtA/+}Per2^{luc/+}$) mice. Raw bioluminescence data were normalized by subtraction of the 24-h running average and then smoothed with a 2-h running average. Note that the first 12 h of raw counts are not included in the normalized data. Data are mean ± SEM (n = 3–4 independent experimental repetitions per genotype/diet using isolated islets from n = 2 mice per genotype/diet). *$P < 0.05$. *D*: *Bmal1*, *Per2*, *Cry1*, and *Nr1d1* mRNA levels obtained from islet lysates of HFD-fed control ($^{+/+}Ins2^{rtTA/+}$) and *β-Bmal1*^{OV} (*Bmal1-HA*$^{tetO/+}$$Ins2^{rtTA/+}$) male mice collected at the ZT 4, 8, 16, and 20 time points in the 24-h circadian cycle. Data are mean ± SEM (n = 3 independent experimental repetitions per ZT/genotype using isolated islets from n = 2–4 mice per ZT/genotype) fold change, with control at ZT 4 set as 1. *$P < 0.05$ vs. control (two-way ANOVA). BF, bright field.

from HFD-fed controls exhibit characteristic features of β-cell dysfunction in T2DM (i.e., increased basal insulin release), loss of first-phase GSIS, and preserved second-phase GSIS ($P < 0.05$ for basal and first phase for chow vs. HFD-control) (Fig. 5). *Bmal1* overexpression attenuated insulin secretory abnormalities by normalizing basal insulin and restoring first-phase insulin response ($P < 0.05$ for *β-Bmal1*^{OV}-HFD vs. control-HFD) (Fig. 5*C*). In contrast, *Bmal1* overexpression had no effect on second-phase insulin response. Of note, improvements of β-cell function and glucose tolerance in HFD-fed *β-Bmal1*^{OV} mice were not associated with changes in β-cell mass or β-cell turnover (e.g., proliferation, apoptosis) ($P > 0.05$ between genotypes for all parameters) (Supplementary Fig. 3).

BMAL1 Overexpression in β-Cells Leads to Enhanced Expression of Genes Regulating Insulin Secretion, ER Function, and Lipid Metabolism

Next, we performed whole-genome analysis of HFD-fed control and *β-Bmal1*^{OV} isolated islets at the ZT 4 and ZT 16 time points (Fig. 6). At ZT 4, pathway analysis of genes enriched in islets of HFD-fed *β-Bmal1*^{OV} mice (twofold increase vs. HFD-fed control) showed enrichment for genes involved in the regulation of insulin secretion, ER insulin processing, and lipid metabolism (e.g., GO:0032787 ~ peptide hormone processing, GO:0030073 ~ insulin secretion, GO:0016485 ~ protein processing) (Fig. 6*B* and Supplementary Material). In contrast, at ZT 16, islets of HFD-fed *β-Bmal1*^{OV} mice showed enrichment of transcripts

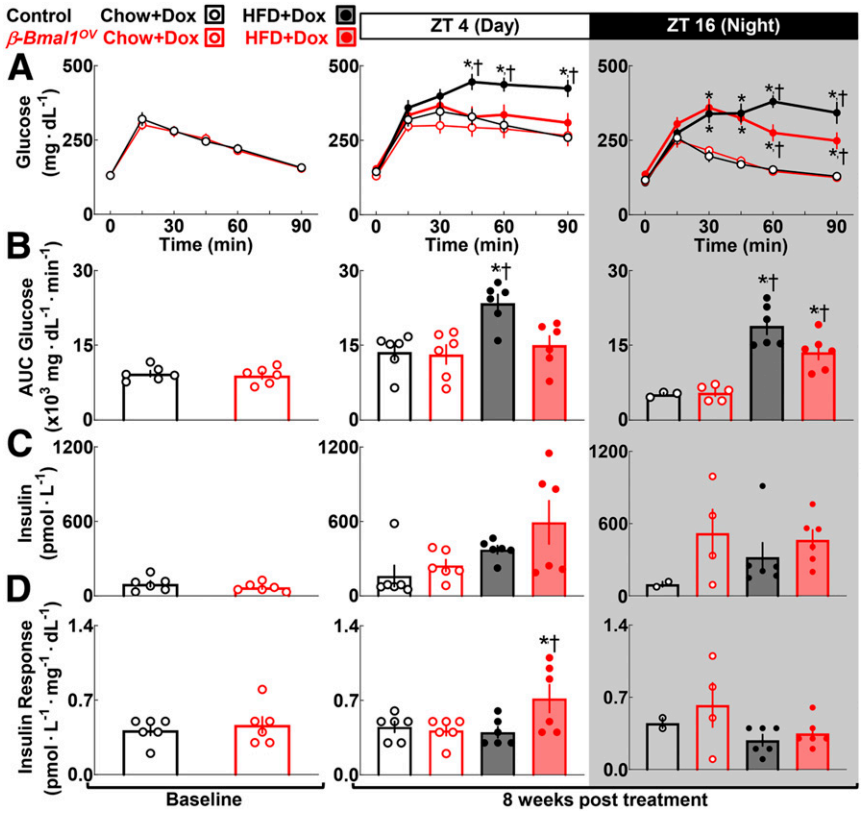

Figure 4—β-Cell *Bmal1* overexpression enhances in vivo glucose tolerance in response to diet-induced obesity in male mice. Graphs depict sampled blood glucose during i.p. GTT (*A*), corresponding glucose AUC during GTT (*B*), plasma insulin collected at 15 min post-glucose administration during GTT (*C*), and corresponding insulin response expressed as insulin/glucose at 15 min post-glucose administration during GTT performed at the ZT 4 and ZT 16 time points in control ($^{+/+}Ins2^{rtTA/+}$) and *β-Bmal1*^{OV} (*Bmal1-HA*$^{tetO/+}$*Ins2*$^{rtTA/+}$) male mice at baseline (2 months of age) and after 8-week exposure to 60% HFD + DOX vs. chow + DOX (*D*). Data are mean ± SEM (n = 6 mice per genotype/diet except as a result of sampling difficulties for insulin/insulin response at ZT 16 for *β-Bmal1*^{OV}-chow and control-chow). *P < 0.05 for diet; †P < 0.05 for genotype.

regulating circadian rhythms and the inflammatory response (e.g., GO:0045087 ~ innate immune response, GO:0034097 ~ response to cytokine, GO:0032922 ~ circadian regulation) (Fig. 6*B* and Supplementary Material). Importantly, GSEA revealed that transcripts upregulated in islets of HFD-fed *β-Bmal1*^{OV} mice (at ZT 4 and ZT 16) were significantly enriched for genes annotated to BMAL1 genomic binding sites previously reported for β-cells (6) (false discovery rate P < 0.0001) (Fig. 6*C*). Furthermore, key findings were confirmed by qRT-PCR, which showed enhanced expression of key islet transcripts regulating GSIS (e.g., *Abcc8*, *Glp1r*), lipid metabolism (e.g., *Fabp1*, *Apoa1*), and insulin processing/folding (e.g., *Ero1b*, *Cpe*) (P < 0.05 for all vs. control) (Fig. 6*D*).

Administration of Nobiletin Enhances Islet Circadian Clock Amplitude and GSIS in Isolated Islets

We next tested whether pharmacological enhancement of the circadian clock amplitude in vitro augments GSIS in isolated mouse and human islets. Polymethoxylated flavone nobiletin has been identified as a potent clock amplitude–enhancing compound (18). Correspondingly, to assess the effect of nobiletin on β-cell circadian clock, we crossed *Per2*:LUC reporter with mice expressing GFP under the control of the insulin promoter (22) ($Per2^{luc/+}Ins1^{GFP/+}$) and examined activation of *Per2*-driven bioluminescence in β-cells in response to nobiletin (10 μmol · L^{-1}) vs. vehicle (DMSO) (Fig. 7*A*–*C*). These studies revealed that nobiletin enhanced the amplitude (~1.5 fold, P < 0.05 vs. DMSO) (Fig. 7*A*) of *Per2*-driven luciferase oscillations, consistent with purported effects of this compound as a clock-enhancing small molecule.

We next tested the ability of nobiletin to modulate insulin secretion in isolated islets using islet perifusion. Administration of nobiletin augmented GSIS in mouse islets by increasing both first- and second-phase insulin response (P < 0.05 vs. DMSO) (Fig. 7*D*–*F*), without altering basal insulin response. Importantly, nobiletin failed to augment GSIS in islets from mice with a conditional β-cell–specific deletion of *Bmal1* (*β-Bmal1*$^{-/-}$), thus confirming that stimulatory effects of nobiletin on insulin secretion were dependent on intact β-cell *Bmal1* expression (Fig. 7*D*–*F*). Finally, we also examined whether nobiletin modulates insulin secretion in nondiabetic and T2DM

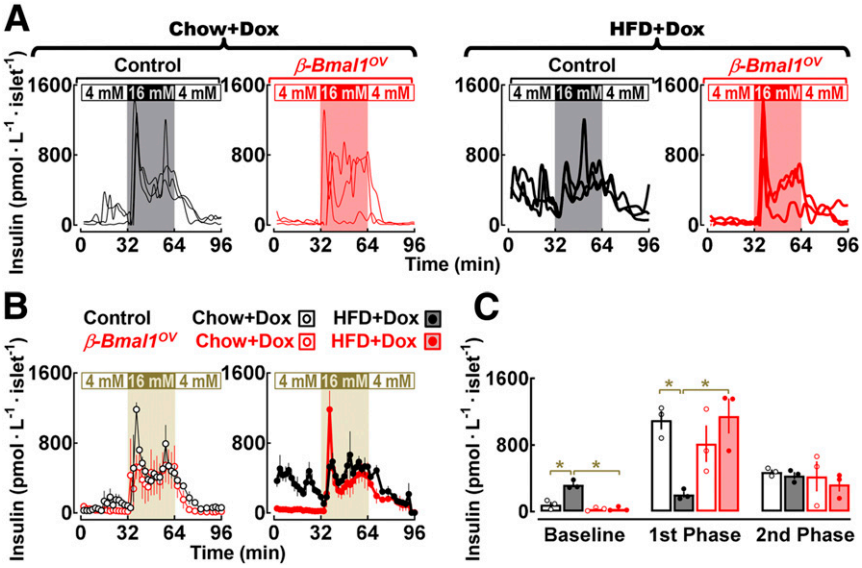

Figure 5—β-Cell *Bmal1* overexpression reverses β-cell functional failure in response to diet-induced obesity in male mice. *A* and *B*: Individual insulin concentration profiles (traces) and corresponding means ± SEMs sampled at 2-min intervals during islet perifusion performed at 4 mmol · L^{-1} glucose (0–32 min), 16 mmol · L^{-1} glucose (32–64 min), and back to 4 mmol · L^{-1} glucose (64–96 min) in islets isolated from chow- and HFD-fed control ($^{+/+}Ins2^{rtTA/+}$) and *β-Bmal1*^{OV} (*Bmal1-HA*$^{tetO/+}$*Ins2*$^{rtTA/+}$) male mice. *C*: Mean basal (mean insulin concentration during 4 mmol · L^{-1} glucose), first-phase (mean first peak insulin concertation at 16 mmol · L^{-1} glucose), and second-phase (mean insulin concentration during 16 mmol · L^{-1} glucose after the first peak) insulin responses during perifusions of islets from chow- and HFD-fed control ($^{+/+}Ins2^{rtTA/+}$) and *β-Bmal1*^{OV} (*Bmal1-HA*$^{tetO/+}$*Ins2*$^{rtTA/+}$) male mice. Data are mean ± SEM (n = 3 independent experimental perifusions per genotype/diet using isolated islets from n = 3 mice per genotype/diet). *$P < 0.05$. mM, mmol · L^{-1}.

human islets (Fig. 8*A–C*). Consistent with the data in mouse islets, nobiletin was able to enhance first- and second-phase insulin response in nondiabetic and T2DM human islets (~1.5–2-fold, $P < 0.05$ vs. DMSO) (Fig. 8*A–C*) without altering basal insulin response.

DISCUSSION

The pathophysiology of β-cell failure in T2DM manifests largely as a result of impaired/insufficient GSIS in the context of prevailing insulin resistance, which is typically associated with obesity (31–33). Thus, mechanisms mediating preservation of β-cell secretory function in the context of obesity and insulin resistance may provide the basis for novel therapeutic strategies. The current study provides evidence that β-cell–specific overexpression of a key circadian transcription factor, BMAL1, enhances circadian clock function and consequently augments GSIS and whole-body glucose metabolism in the context of diet-induced obesity.

Accumulating epidemiological, clinical, and animal studies have demonstrated functional links between circadian disruption and development of T2DM (9,10). Importantly, this relationship is mediated at least in part through circadian disruption of pancreatic β-cell functionality (9), suggesting that misregulation of the circadian system may play an important role in the induction of β-cell failure in T2DM (12). This postulate is supported by *Bmal1* genetic loss-of-function studies, which have collectively demonstrated the importance of *Bmal1* in the regulation of β-cell maturation (8), GSIS and glucose tolerance (3,6,34), β-cell turnover (16), mitochondrial function (7), and response to oxidative/ER stress (15). Consistently, in humans, *Bmal1* genetic variants are associated with development of T2DM (17), and impaired circadian insulin secretion is a feature of T2DM (12,35).

Given the critical function of BMAL1 in the regulation of insulin secretion and β-cell response to diabetogenic stressors, we first tested whether conditional overexpression of *Bmal1* in β-cells results in metabolic protection against diet-induced obesity. We used a genetic approach by generating double-transgenic mice with β-cell–specific inducible expression of BMAL1, which was first used for selective rescue of BMAL1 expression in the suprachiasmatic nucleus of the hypothalamus and skeletal muscle of *Bmal1* knockout mice (20). Consistently, we observed robust β-cell–specific *Bmal1* overexpression at the mRNA and protein level. We also confirmed functionality of tetracycline-driven BMAL1 by assessing *Per2*:LUC reporter activity in isolated islets of triple-transgenic mice expressing *Bmal1*$^{tetO/+}$*Ins2*$^{rtTA/+}$*Per2*$^{luc/+}$. Most notably, *β-Bmal1*^{OV} mice were protected from obesity-induced glucose intolerance attributed to enhanced first-phase insulin response and attenuated basal insulin hypersecretion.

Our results also show that the clock-enhancing compound nobiletin increased islet circadian clock amplitude and augmented GSIS in isolated mouse and human islets in a *Bmal1*-dependent manner. He et al. (18) used an unbiased chemical screen to identify nobiletin as a clock-enhancing compound that activates retinoid acid receptor–related orphan (RORα), which is a known transcriptional

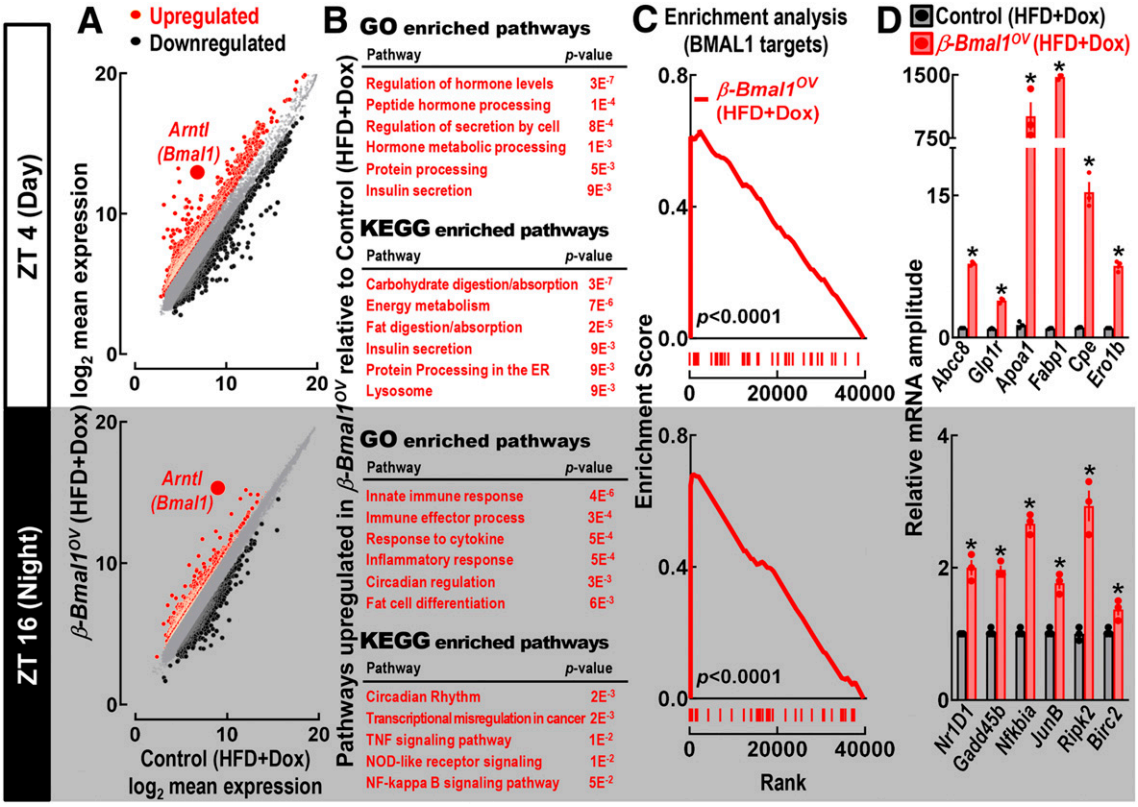

Figure 6—β-Cell *Bmal1* overexpression leads to enhanced circadian expression of transcripts regulating lipid metabolism, ER function, and insulin secretion in male mice. *A*: Scatter plots showing biweight $\log_2$ average expression values from Affymetrix GeneChip of all genes in HFD-fed control ($^{+/+}Ins2^{rtTA/+}$) and *β-Bmal1*^{OV} (*Bmal1-HA*$^{tetO/+}$*Ins2*$^{rtTA/+}$) islets at the ZT 4 and ZT 16 time points. Gray circles indicate unchanged expression, red circles represent upregulated genes, and black circles represent downregulated genes, with fold regulation cutoff set at 2. Expression level of *Arntl* (*Bmal1*) is shown as a large red circle. For Affymetrix GeneChip, islets were isolated from seven control-HFD ($n = 3$ at ZT 4 and $n = 4$ at ZT 16) and eight *β-Bmal1*^{OV}-HFD ($n = 5$ at ZT 4 and $n = 3$ at ZT 16) mice. To maximize the amount and quality of RNA, islet samples were pooled to create a sample for each genotype/ZT. *B*: Tables showing significantly upregulated GO biological processes and Kyoto Encyclopedia of Genes and Genomes (KEGG) pathways with a $P < 0.05$ in HFD-fed *β-Bmal1*^{OV} vs. control islets at the ZT 4 and ZT 16 time points. *C*: GSEA performed using preranked analysis of genes previously annotated to BMAL1 genomic binding cites (6) (false discovery rate $P < 0.0001$). *D*: Confirmation of key upregulated transcripts from Affymetrix GeneChip by qRT-PCR in HFD-fed *β-Bmal1*^{OV} vs. control islets at the ZT 4 and ZT 16 time points. Data are mean ± SEM ($n = 3$ independent experimental repetitions per ZT/genotype using isolated islets from $n = 3$ mice per ZT/genotype). *$P < 0.05$ vs. control.

activator of *Bmal1*. Importantly, studies have shown beneficial effects of nobiletin administration on glucose tolerance in animal models of obesity and diabetes (18). Furthermore, consistent with our observations, nobiletin has been recently shown to enhance molecular circadian rhythms, insulin secretion, and protect from oxidative stress in isolated human islets (12,36).

To identify a potential molecular basis behind our observations, we examined diurnal gene expression in islets of control and *β-Bmal1*^{OV} mice. Consistent with improved diurnal glucose tolerance, basal hypersecretion, and GSIS, islets of obese *β-Bmal1*^{OV} mice exhibited increased expression of genes involved in the regulation of insulin secretion, insulin processing, circadian rhythms, and lipid metabolism. An enrichment for genes regulating insulin secretion and ER function is particularly interesting given the critical role of these processes in maintaining β-cell functionality in response to obesity, hyperlipidemia, and insulin resistance (37–39). Indeed, insulin resistance states have been shown to promote β-cell secretory dysfunction and loss of transcriptional identity by compromising insulin processing and ER function (37,38,40). Moreover, islets of obese *β-Bmal1*^{OV} also demonstrated upregulation of genes regulating lipid transport and metabolism (e.g., *Fabp1*, *Apoa1*), which is in concert with reports suggesting the role of these genes in lipotoxicity and β-cell viability (41).

Recent studies have suggested that the ability (and tissue/cell-type specificity) of BMAL1 DNA binding and transcriptional activation depends on chromatin accessibility and cobinding with tissue-specific transcription factors (14). In β-cells, BMAL1 DNA binding and activation of circadian transcription occur within distal tissue-specific enhancers and are associated with cobinding by key β-cell transcription factor PDX1 (6). Although our study did not directly assess the dynamics of BMAL1 DNA binding, GSEA revealed that transcripts upregulated in islets of *β-Bmal1*^{OV} mice were enriched for genes annotated as

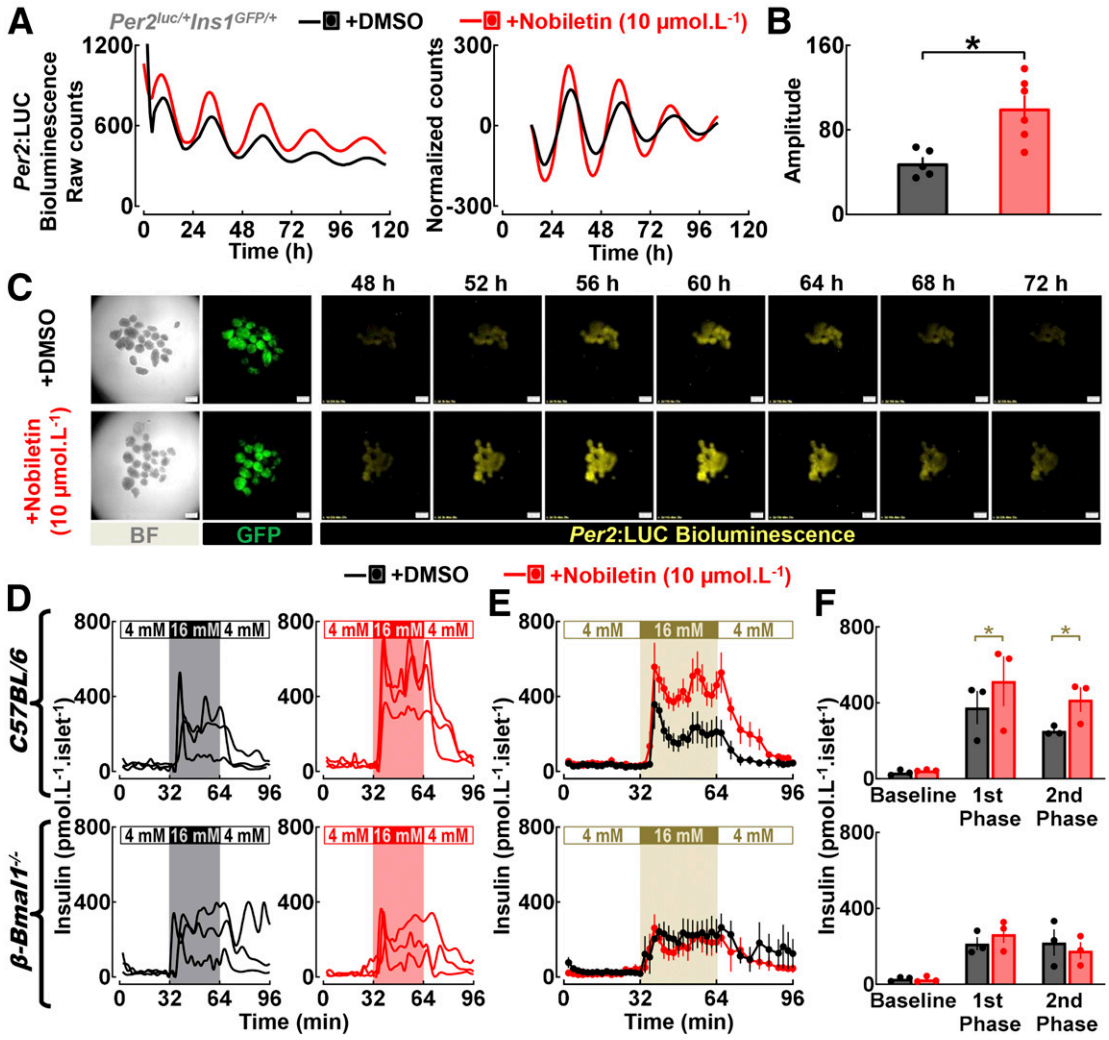

Figure 7—Administration of clock-modifying compound nobiletin enhances islet circadian clock amplitude and GSIS in isolated male mouse islets. *A–C*: Representative examples of *Per2*-driven bioluminescence rhythms (raw and normalized counts) (*A*), mean circadian amplitude of *Per2*-driven bioluminescence rhythms (*B*), and 24 h of time-lapse microscopy recordings (scale bars = 200 μm) (*C*) in islets isolated from $Per2^{luc/+}Ins1^{GFP/+}$ mice exposed in vitro to either nobiletin (10 μmol · L^{-1}) or vehicle (DMSO). Islets were continuously exposed to nobiletin (10 μmol · L^{-1}) throughout the duration of bioluminescence recordings (0–120 h). Raw bioluminescence data were normalized by subtraction of the 24-h running average and then smoothed with a 2-h running average. Note that the first 12 h of raw counts are not included in the normalized data. Data are mean ± SEM (n = 4–6 independent experimental repetitions per condition [i.e., nobiletin vs. DMSO] using isolated islets from n = 3 mice). *$P < 0.05$ vs. DMSO. *D* and *E*: Individual insulin concentration profiles and corresponding means ± SEMs sampled at 2-min intervals at 4 mmol · L^{-1} glucose (0–32 min), 16 mmol · L^{-1} glucose (32–64 min), and back to 4 mmol · L^{-1} glucose (64–96 min) in islets isolated from male C57BL/6J mice (n = 3) and mice with a conditional β-cell–specific deletion of *Bmal1* (β-$Bmal1^{-/-}$) (n = 3) exposed to either nobiletin (10 μmol · L^{-1}, n = 3 independent perifusion runs) or vehicle (DMSO, n = 3 perifusion runs). Nobiletin (10 μmol · L^{-1}) was diluted in 4 mmol · L^{-1} and 16 mmol · L^{-1} glucose perifusion buffer and was continuously administered throughout the basal wash (−48 to 0 min) and sample collection (0–96 min) period of islet perifusion. *F*: Mean basal (mean insulin concentration during 4 mmol · L^{-1} glucose), first-phase (mean first peak insulin concentration at 16 mmol · L^{-1} glucose), and second-phase (mean insulin concentration during 16 mmol · L^{-1} glucose after the first peak) insulin responses during perifusions of islets isolated from male C57BL/6J mice (n = 3) and mice with a conditional β-cell–specific deletion of *Bmal1* (β-$Bmal1^{-/-}$) (n = 3) exposed to either nobiletin (10 μmol · L^{-1}, n = 3 perifusion runs) or vehicle (DMSO, n = 3 perifusion runs). *$P < 0.05$. BF, bright field; mM, mmol · L^{-1}.

BMAL1 genomic binding sites in β-cells (6). It is also important to acknowledge that β-$Bmal1^{OV}$-driven changes in the genome may also be attributed to global reduction in cellular oxidative and ER stress, previously shown to be regulated through BMAL1-mediated expression of a key antioxidative stress transcription factor *Nrf2* (15). In this regard, attenuated basal hypersecretion in obese β-$Bmal1^{OV}$ is noteworthy, given that elevated basal insulin is an important feature of stressed β-cells in T2DM (31,32).

It is also important to acknowledge some limitations of our study. The use of Ins2-driven rtTA mice presents a limitation because of potential activity of this promoter

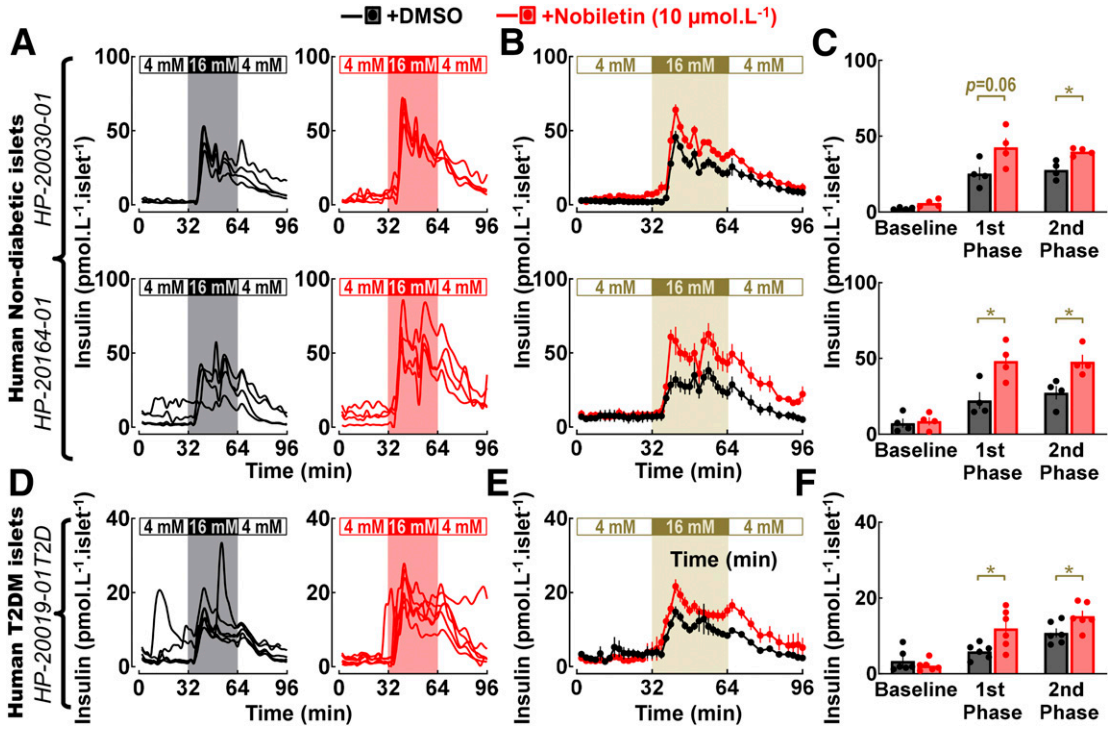

Figure 8—Administration of clock-modifying compound nobiletin enhances GSIS in isolated nondiabetic and T2DM human islets. Individual insulin concentration profiles (*A* and *D*) and corresponding means ± SEMs (*B* and *E*) sampled at 2-min intervals during islet perifusion performed at 4 mmol · L^{-1} glucose (0–32 min), 16 mmol · L^{-1} glucose (32–64 min), and back to 4 mmol · L^{-1} glucose (64–96 min) in isolated cadaveric human nondiabetic and T2DM islets exposed during perifusion to either nobiletin (10 μmol · L^{-1}) or vehicle (DMSO). Nobiletin (10 μmol · L^{-1}) was diluted in 4 mmol · L^{-1} and 16 mmol · L^{-1} glucose perifusion buffer and was continuously administered throughout the basal wash (−48 to 0 min) and sample collection (0–96 min) period of islet perifusion. In total, two independent shipments of nondiabetic (HP-20030 and HP-20164) and one shipment of T2DM (HP-20019) human islets were used, and means ± SEMs for each islet shipment were derived from $n = 4$–6 independent experimental repetitions per condition (i.e., nobiletin vs. DMSO). Mean basal (mean insulin concentration during 4 mmol · L^{-1} glucose), first-phase (mean first peak insulin concertation at 16 mmol · L^{-1} glucose), and second-phase (mean insulin concentration during 16 mmol · L^{-1} glucose after the first peak) insulin responses during perifusions of cadaveric human nondiabetic and T2DM islets exposed to either nobiletin (10 μmol · L^{-1}) or vehicle (DMSO) (*C* and *F*). Data are mean ± SEM for each islet shipment derived from $n = 4$–6 independent experimental repetitions per condition (i.e., nobiletin vs. DMSO). *$P < 0.05$. mM, mmol · L^{-1}.

in the hypothalamus. Although we cannot rule out this possibility, we did not observe alterations in global behavioral or metabolic circadian rhythms in *β-Bmal1*^{OV} mice. Moreover, previous studies using this model failed to observe DOX-mediated alterations in hypothalamic gene expression (42). In addition, the majority of experimental outcomes in our study were obtained at two diurnal time points (e.g., ZT 4, ZT 16), which were chosen to represent a previously observed trough and peak of *Bmal1* expression in mouse islets (43). This approach, however, precluded us from characterizing endogenous circadian rhythms, which requires more frequent sampling periodicity. Finally, lack of detailed characterization of in vivo GSIS in *β-Bmal1*^{OV} mice is another limitation of the study. Although islet perifusion data show robust improvements in GSIS of *β-Bmal1*^{OV} mice, future studies will be required to characterize in vivo insulin secretion in response to genetic and pharmacological agonism of the β-cell circadian clock.

In summary, evidence suggests that development of obesity and T2DM is characterized by disrupted circadian physiology and impaired function of intracellular circadian clocks (9,10,12). Thus, therapeutic strategies designed to enhance circadian clock function may be beneficial for prevention and treatment of T2DM. Consistently, our studies support the hypothesis that circadian clock–enhancing strategies may be effective in counteracting β-cell functional failure. However, given temporal differences in the phase of circadian clock gene expression in different tissues, future studies will be required to test the efficacy and target tissue specificity of circadian clock modifiers as a potential treatment of diabetes.

Acknowledgments. The authors thank Matthew R. Brown and Asha Nair (Mayo Clinic) for helpful discussions and suggestions with bioinformatics analyses. The authors also acknowledge Nathan K. LeBrasseur and Thomas White (Mayo Clinic Robert and Arlene Kogod Center on Aging) for assistance and interpretation of energy expenditure data.

Funding. The authors acknowledge funding support from the National Institutes of Health Center for Scientific Review (2R01-DK-098468 to A.V.M.) and the Center for Regenerative Medicine (Mayo Clinic).

Duality of Interest. No potential conflicts of interest relevant to this article were reported.

Author Contributions. K.R. contributed to the study design, conducted the experiments, performed the data analysis, and assisted with preparation of the

manuscript. A.V.M. designed and interpreted the studies and wrote the manuscript. A.V.M. is the guarantor of this work and, as such, had full access to all data in the study and takes responsibility for the integrity of the data and the accuracy of the data analysis.

References

1. Pittendrigh CS. Temporal organization: reflections of a Darwinian clock-watcher. Annu Rev Physiol 1993;55:16–54
2. Takahashi JS. Transcriptional architecture of the mammalian circadian clock. Nat Rev Genet 2017;18:164–179
3. Marcheva B, Ramsey KM, Buhr ED, et al. Disruption of the clock components CLOCK and BMAL1 leads to hypoinsulinaemia and diabetes. Nature 2010;466:627–631
4. Petrenko V, Saini C, Giovannoni L, et al. Pancreatic α- and β-cellular clocks have distinct molecular properties and impact on islet hormone secretion and gene expression. Genes Dev 2017;31:383–398
5. Pulimeno P, Mannic T, Sage D, et al. Autonomous and self-sustained circadian oscillators displayed in human islet cells. Diabetologia 2013;56:497–507
6. Perelis M, Marcheva B, Ramsey KM, et al. Pancreatic β cell enhancers regulate rhythmic transcription of genes controlling insulin secretion. Science 2015;350:aac4250
7. Lee J, Moulik M, Fang Z, et al. Bmal1 and β-cell clock are required for adaptation to circadian disruption, and their loss of function leads to oxidative stress-induced β-cell failure in mice. Mol Cell Biol 2013;33:2327–2338
8. Rakshit K, Qian J, Gaonkar KS, Dhawan S, Colwell CS, Matveyenko AV. Postnatal ontogenesis of the islet circadian clock plays a contributory role in β-cell maturation process. Diabetes 2018;67:911–922
9. Perelis M, Ramsey KM, Marcheva B, Bass J. Circadian transcription from beta cell function to diabetes pathophysiology. J Biol Rhythms 2016;31:323–336
10. Javeed N, Matveyenko AV. Circadian etiology of type 2 diabetes mellitus. Physiology (Bethesda) 2018;33:138–150
11. Qian J, Scheer FAJL. Circadian system and glucose metabolism: implications for physiology and disease. Trends Endocrinol Metab 2016;27:282–293
12. Petrenko V, Gandasi NR, Sage D, Tengholm A, Barg S, Dibner C. In pancreatic islets from type 2 diabetes patients, the dampened circadian oscillators lead to reduced insulin and glucagon exocytosis. Proc Natl Acad Sci U S A 2020;117:2484–2495
13. Bunger MK, Wilsbacher LD, Moran SM, et al. Mop3 is an essential component of the master circadian pacemaker in mammals. Cell 2000;103:1009–1017
14. Beytebiere JR, Trott AJ, Greenwell BJ, et al. Tissue-specific BMAL1 cistromes reveal that rhythmic transcription is associated with rhythmic enhancer-enhancer interactions. Genes Dev 2019;33:294–309
15. Lee J, Liu R, de Jesus D, et al. Circadian control of β-cell function and stress responses. Diabetes Obes Metab 2015;17(Suppl. 1):123–133
16. Rakshit K, Hsu TW, Matveyenko AV. Bmal1 is required for beta cell compensatory expansion, survival and metabolic adaptation to diet-induced obesity in mice. Diabetologia 2016;59:734–743
17. Woon PY, Kaisaki PJ, Bragança J, et al. Aryl hydrocarbon receptor nuclear translocator-like (BMAL1) is associated with susceptibility to hypertension and type 2 diabetes. Proc Natl Acad Sci U S A 2007;104:14412–14417
18. He B, Nohara K, Park N, et al. The small molecule nobiletin targets the molecular oscillator to enhance circadian rhythms and protect against metabolic syndrome. Cell Metab 2016;23:610–621
19. Thomas AP, Hoang J, Vongbunyong K, Nguyen A, Rakshit K, Matveyenko AV. Administration of melatonin and metformin prevents deleterious effects of circadian disruption and obesity in male rats. Endocrinology 2016;157:4720–4731
20. McDearmon EL, Patel KN, Ko CH, et al. Dissecting the functions of the mammalian clock protein BMAL1 by tissue-specific rescue in mice. Science 2006;314:1304–1308
21. Nir T, Melton DA, Dor Y. Recovery from diabetes in mice by beta cell regeneration. J Clin Invest 2007;117:2553–2561
22. Hara M, Wang X, Kawamura T, et al. Transgenic mice with green fluorescent protein-labeled pancreatic beta -cells. Am J Physiol Endocrinol Metab 2003;284:E177–E183
23. Storch KF, Paz C, Signorovitch J, et al. Intrinsic circadian clock of the mammalian retina: importance for retinal processing of visual information. Cell 2007;130:730–741
24. Dor Y, Brown J, Martinez OI, Melton DA. Adult pancreatic beta-cells are formed by self-duplication rather than stem-cell differentiation. Nature 2004;429:41–46
25. Costes S, Boss M, Thomas AP, Matveyenko AV. Activation of melatonin signaling promotes β-cell survival and function. Mol Endocrinol 2015;29:682–692
26. Qian J, Block GD, Colwell CS, Matveyenko AV. Consequences of exposure to light at night on the pancreatic islet circadian clock and function in rats. Diabetes 2013;62:3469–3478
27. Qian J, Yeh B, Rakshit K, Colwell CS, Matveyenko AV. Circadian disruption and diet-induced obesity synergize to promote development of β-cell failure and diabetes in male rats. Endocrinology 2015;156:4426–4436
28. Huang DW, Sherman BT, Tan Q, et al. The DAVID Gene Functional Classification Tool: a novel biological module-centric algorithm to functionally analyze large gene lists. Genome Biol 2007;8:R183
29. Hughes ME, Hogenesch JB, Kornacker K. JTK_CYCLE: an efficient nonparametric algorithm for detecting rhythmic components in genome-scale data sets. J Biol Rhythms 2010;25:372–380
30. Yoo SH, Yamazaki S, Lowrey PL, et al. PERIOD2:LUCIFERASE real-time reporting of circadian dynamics reveals persistent circadian oscillations in mouse peripheral tissues. Proc Natl Acad Sci U S A 2004;101:5339–5346
31. Cohrs CM, Panzer JK, Drotar DM, et al. Dysfunction of persisting β cells is a key feature of early type 2 diabetes pathogenesis. Cell Rep 2020;31:107469
32. Erion K, Corkey BE. β-cell failure or β-cell abuse? Front Endocrinol (Lausanne) 2018;9:532
33. Kahn SE, Zraika S, Utzschneider KM, Hull RL. The beta cell lesion in type 2 diabetes: there has to be a primary functional abnormality. Diabetologia 2009;52:1003–1012
34. Sadacca LA, Lamia KA, deLemos AS, Blum B, Weitz CJ. An intrinsic circadian clock of the pancreas is required for normal insulin release and glucose homeostasis in mice. Diabetologia 2011;54:120–124
35. Boden G, Chen X, Polansky M. Disruption of circadian insulin secretion is associated with reduced glucose uptake in first-degree relatives of patients with type 2 diabetes. Diabetes 1999;48:2182–2188
36. Keshtkar S, Kaviani M, Jabbarpour Z, et al. Protective effect of nobiletin on isolated human islets survival and function against hypoxia and oxidative stress-induced apoptosis. Sci Rep 2019;9:11701
37. Alarcon C, Boland BB, Uchizono Y, et al. Pancreatic β-cell adaptive plasticity in obesity increases insulin production but adversely affects secretory function. Diabetes 2016;65:438–450
38. Arunagiri A, Haataja L, Pottekat A, et al. Proinsulin misfolding is an early event in the progression to type 2 diabetes. eLife 2019;8:e44532
39. Jang I, Pottekat A, Poothong J, et al. PDIA1/P4HB is required for efficient proinsulin maturation and ß cell health in response to diet induced obesity. eLife 2019;8:e44528
40. Kaufman RJ, Back SH, Song B, Han J, Hassler J. The unfolded protein response is required to maintain the integrity of the endoplasmic reticulum, prevent oxidative stress and preserve differentiation in β-cells. Diabetes Obes Metab 2010;12(Suppl. 2):99–107
41. Ye R, Wang M, Wang QA, Scherer PE. Adiponectin-mediated antilipotoxic effects in regenerating pancreatic islets. Endocrinology 2015;156:2019–2028
42. Pullen TJ, Sylow L, Sun G, Halestrap AP, Richter EA, Rutter GA. Overexpression of monocarboxylate transporter-1 (SLC16A1) in mouse pancreatic β-cells leads to relative hyperinsulinism during exercise. Diabetes 2012;61:1719–1725
43. Rakshit K, Qian J, Ernst J, Matveyenko AV. Circadian variation of the pancreatic islet transcriptome. Physiol Genomics 2016;48:677–687